ARTICLES

Journal of Semiconductors
(2019) 40, 112601
doi: 10.1088/1674-4926/40/11/112601

Screen-printed soft triboelectric nanogenerator with porous PDMS and stretchable PEDOT:PSS electrode

Haochuan Wan[1], Yunqi Cao[2], Li-Wei Lo[1, 3], Zhihao Xu[1], Nelson Sepúlveda[2], and Chuan Wang[1, 3, †]

[1]Electrical and Systems Engineering, Washington University in St. Louis, St Louis, Missouri 63130, United States

[2]Electrical and Computer Engineering, Michigan State University, East Lansing, Michigan 48824, United States

[3]Institute of Materials Science and Engineering, Washington University in St. Louis, St. Louis, Missouri 63130, United States

Abstract: The recent development on wearable and stretchable electronics calls for skin conformable power sources that are beyond current battery technologies. Among the many novel energy devices being explored, triboelectric nanogenerator (TENG) made from intrinsically stretchable materials has a great potential to meet the above requirement as being both soft and efficient. In this paper, we present a lithography-free and low-cost TENG device comprising a porous-structured PDMS layer and a stretchable PEDOT:PSS electrode. The porous PDMS structure is formed by using self-assembled polystyrene beads as the sacrificial template and it is highly ordered with great uniformity and high structural stability under compression force. Moreover, the porous PDMS TENG exhibits improved output voltage and current of 1.65 V and 0.54 nA compared to its counterpart with non-porous PDMS with 0.66 V and 0.34 nA. The effect of different loading force and frequency on the output response of the TENG device has also been studied. This work could shed light on diverse structural modification methods for improving the performance of PDMS-based TENG and the development of intrinsically stretchable TENG for wearable device applications.

Key words: triboelectric nanogenerator (TENG); porous PDMS; stretchable materials; wearable electronics

Citation: H C Wan, Y Q Cao, L W Lo, Z H Xu, N Sepúlveda, and C Wang, Screen-printed soft triboelectric nanogenerator with porous PDMS and stretchable PEDOT:PSS electrode[J]. *J. Semicond.*, 2019, 40(11), 112601. http://doi.org/10.1088/1674-4926/40/11/112601

1. Introduction

Rapid growth in the wearable electronics market has led to tremendous amount of new scientific discoveries and technological developments recently. The flexible electronics and stretchable electronics technologies have been extensively studied for applications in flexible/stretchable display[1–3], smart sensing and health care devices[4–7], soft bionic devices[8] and many more. Despite the significant progress, one of the bottlenecks that researchers are still striving to address is the power source issue, which has limited the wearable device applications to a certain extent. For example, for wearable health care devices that are designed to be soft and can conformably adapt to human skin, not only the sensors and electronic circuits but also the power source needs to be soft and compliant, which is beyond the capability of existing industrial battery technologies. Soft nanogenerators based on piezoelectric[9], ferroelectret[10, 11] or triboeletric[12] effect, on the other hand, have been demonstrated to be highly efficient, sustainable, and low-cost energy sources for powering the wearable devices. Such nanogenerators can scavenge the ambient mechanical energy from ubiquitous human motion and convert the harvested energy into electricity. Among them, triboelectric nanogenerator (TENG) has stood out due to its high output voltage and biocompatibility. In addition, compared with traditional electromagnetic generators (EMGs), TENG also exhibits high efficiency in converting low frequency motion mechanical energy into electricity[13]. Moreover, the TENG structure offers an extremely wide range of triboelectric material choices[14], which renders it possible to fabricate intrinsically stretchable TENG devices by simply combining elastic triboelectric materials with stretchable conductors.

Among various stretchable triboelectric materials, elastomer polydimethylsiloxane (PDMS) has been widely used in wearable TENG applications due to its high electronegativity, biocompatibility and simple processing[15, 16]. In order to increase the surface charge density, the surface of PDMS is usually texturized and one commonly studied method is the introduction of micro-sized protruding structure patterned by microfabrication[17, 18]. Nonetheless, due to the use of microfabrication, this method is limited by the sophisticated pattern design and size of wafer. Alternatively, porous PDMS film made from self-assembled microparticle template has also been demonstrated to be an effective way to further enhance the output performances of PDMS-based TENG[19]. Fabricated through a solution-based self-assembly process, such porous structure can be made over large area at extremely low cost and its structure could potentially lead to both increased surface area for friction and increased surface charge density, both of which are desirable properties for high-performance TENG applications.

In this work, we demonstrate a PDMS-based TENG device with screen-printed stretchable electrode and porous PDMS thin film formed by using self-assembled polystyrene beads

Correspondence to: C Wang, chuanwang@wustl.edu
Received 9 AUGUST 2019; Revised 26 SEPTEMBER 2019.

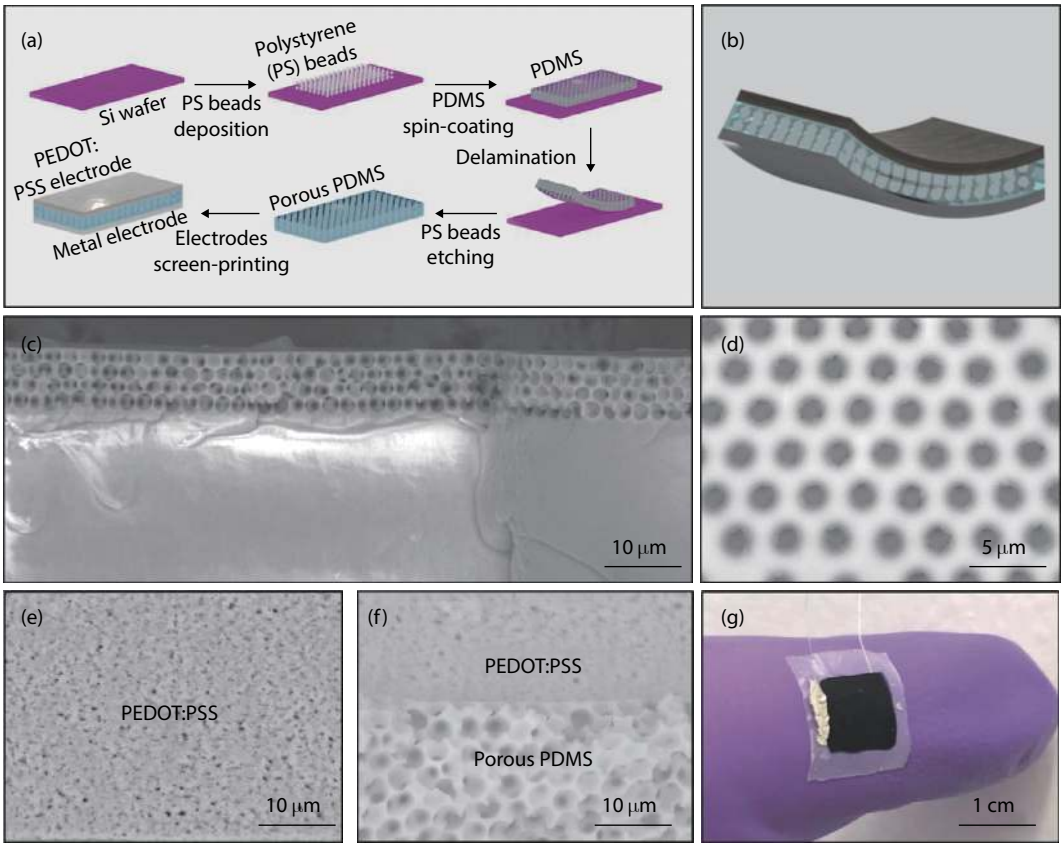

Fig. 1. (Color online) (a) Schematic illustration of the fabrication process of porous PDMS TENG device. (b) Schematic illustration of structure of porous PDMS TENG device. SEM images of porous PDMS thin film from (c) cross-sectional view and (d) top view. SEM images of (e) PEDOT:PSS electrode (f) PEDOT:PSS/Porous PDMS interface. (g) Photograph of fabricated porous PDMS TENG.

as the sacrificial template. The conductive polymer poly(3,4-ethylenedioxythiophene) polystyrene sulfonate (PEDOT:PSS) mixed with bis(trifluoromethane)sulfonimide lithium salt was used as the stretchable conductor and screen-printed onto the porous PDMS, which serves as both the contacting surface and as an electrode. Compared to similar TENG device made with non-porous PDMS, we have observed 2.5 times improvement in output voltage and 1.6 times improvement in output current. The scalable and low-cost fabrication process and great performance offered by the porous PDMS TENG makes it promising for a wide range of applications in wearable energy harvesting devices or sensors.

2. Experiments

Schematic diagrams illustrating the fabrication processes and photographic images of porous PDMS TENG are illustrated in Figs. 1(a), 1(b) and 1(g). 50 μL of polystyrene (PS) latex microspheres water dispersion (6 μm, 2.5 wt%, Alfa Aesar) was drop-casted on Si substrate (1.2 × 1.2 cm^2), followed by heat treatment at 65 °C for 30 min to completely evaporate the solvent. A thin-layer (~100 μm) of PDMS (Dow Corning, Sylgard 184, 10 : 1) was then spin-coated (1000 rpm, 60 s) on the sample and heated on a heating plate at 80 °C for 2.5 h to cure the PDMS. After the PDMS thin film was cured, the sample was immersed in acetone briefly to detach the PS/PDMS thin film from the handling Si substrate. The fabrication of the porous PDMS thin film was completed by completely etching away the PS beads encompassed by PDMS. This was done by exposing the PS-containing side of the PDMS thin film to O_2 plasma treatment (30 W, 15 s), followed by bath sonication in dimethylformamide (DMF) for 3 h and immersion in DMF at room temperature for 12 h. Figs. 1(c) and 1(d) are the cross-sectional view and top view scanning electron microscopy (SEM; JEOL, JEM-7001 LV) images of the porous PDMS thin film. The results show that highly-ordered, multilayer porous PDMS structure was successfully obtained.

The composite PEDOT:PSS ink was prepared by mixing commercial PEDOT:PSS conductive screen printable ink (5 wt%, Sigma-Aldrich, Inc) with 10 wt% of bis(trifluoromethane) sulfonimide lithium salt (Sigma-Aldrich, Inc) and stirring for 15 min to further increase its stretchability[20]. Next, the PEDOT:PSS electrode was screen-printed on the porous side of the porous PDMS film using a PET (Grafix, Inc.) shadow mask with opening of 8 × 8 mm^2 in area and 0.3 mm in thickness. The printed PEDOT:PSS electrode was then cured at 70 °C for 1 h. The SEM images of PEDOT:PSS and its interface with porous PDMS are shown in Figs. 1(e) and 1(f), respectively. After the PEDOT:PSS electrode was cured, one edge of the electrode was connected to a leading wire using silver paint (PELCO 16062, Ted Pella, Inc.) as the adhesive. A metal electrode was fabricated on the other side (non-porous side) of the porous PDMS film using conductive nickel paste (841AR, Super Shield, Inc.) following the similar printing and wiring processes. In order to understand the effect of having porous PDMS structure on the performance of the TENG, a reference sample with entire non-porous PDMS film of the same thickness and the same device structure was also fabricated

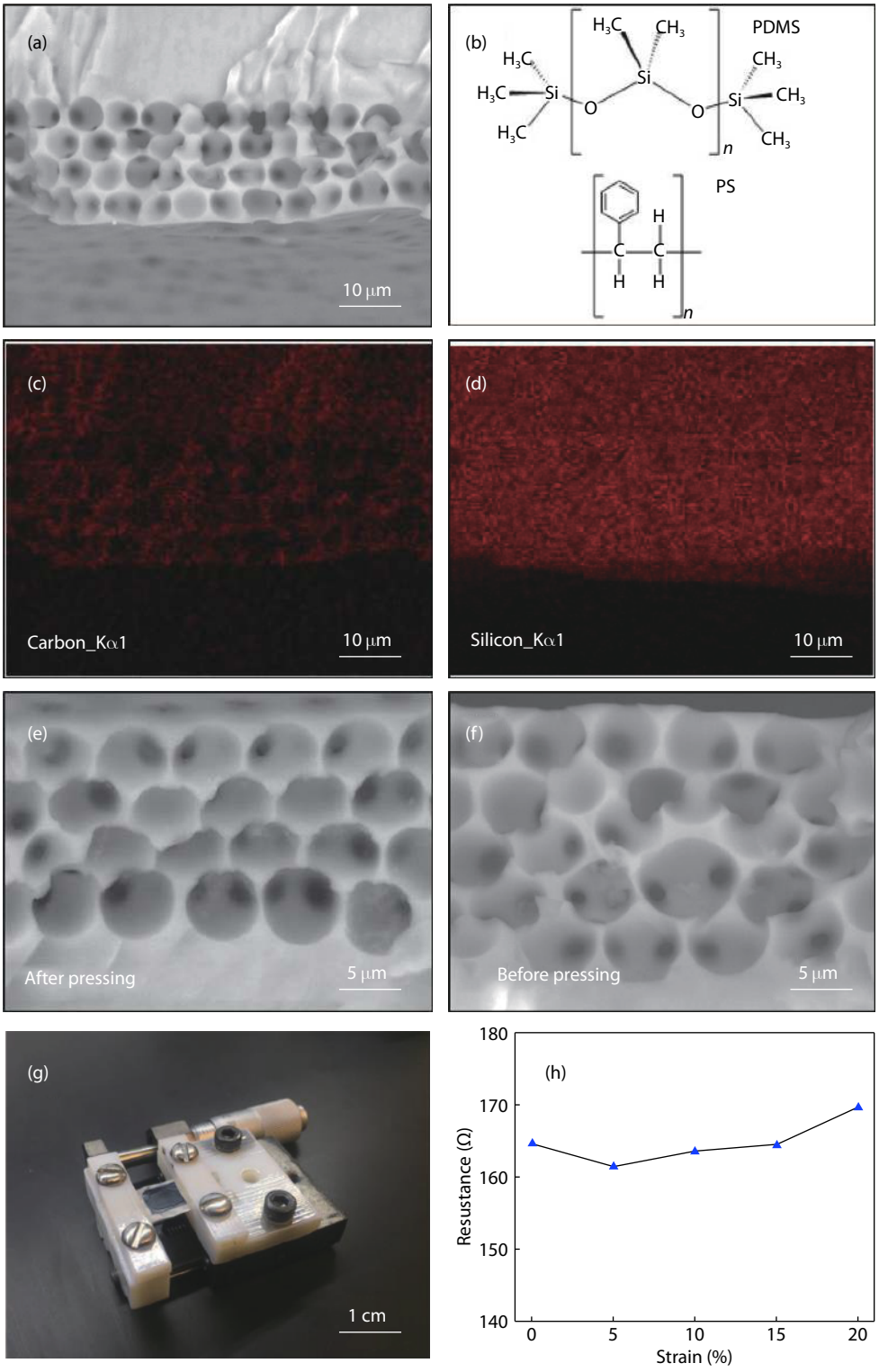

Fig. 2. (Color online) (a) SEM image of porous PDMS structure examined in EDX (b) structural formula of polydimethylsiloxane (PDMS) and polystyrene (PS). Energy dispersive X-ray analysis (EDX) images of (c) carbon element and (d) silicon element of porous PDMS structure. SEM images of porous PDMS structure (e) after compressive pressure (f) before compressive pressure. (g) Photograph of the stretching test setup. (h) Resistance change of the screen-printed PEDOT:PSS electrode under various levels of applied strain.

following the processes above.

3. Results and discussion

To confirm the template formed by PS beads has been completely etched away in the porous structure, energy dispersive X-ray analysis (EDX; JEOL, JEM-7001 LV) was conducted to the cross-sessional area of the porous PDMS structure shown in Fig. 2(a). Structural formula of PDMS and PS shown in Fig. 2(b) suggest the element content of carbon in PS (92.3 wt%) is much higher than PDMS (32.4 wt%) while the element content of silicon in PDMS is 37.8 wt% and in PS is essentially zero. EDX analysis results in Figs. 2(c) and 2(d) indicate that the voids in Fig. 2(a) have nearly zero carbon content while the silicon content is similar to the background PDMS, which suggests that all PS beads have been completely etched away in the porous PDMS structure. It is also

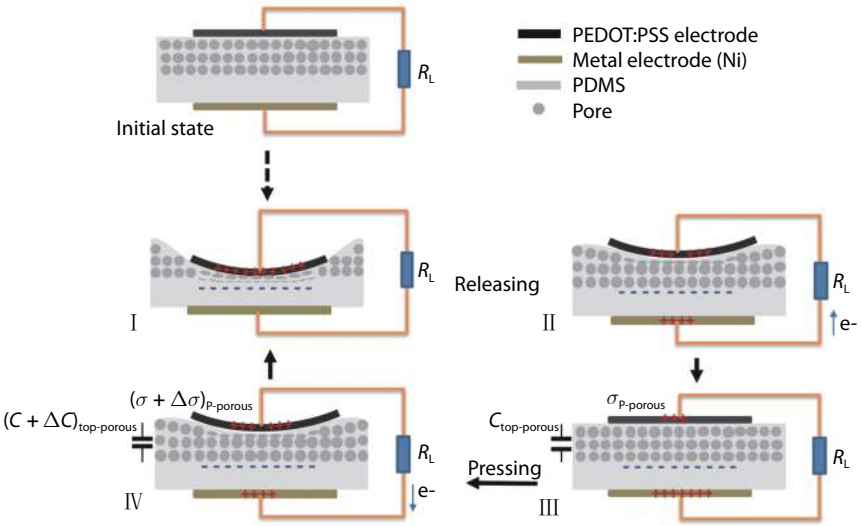

Fig. 3. (Color online) Charge generation mechanism of the porous PDMS TENG under external compressive force.

worth noting that the fabricated porous PDMS structure remains elastic and is highly resilient to compressive strain. SEM images of the porous PDMS cross-sectional structure before (Fig. 2(f)) and after (Fig. 2(e)) pressure of up to 43.6 kPa was applied show the porous structure was fully retained after compression. The electrical property and stretchability of the screen-printed composite PEDOT:PSS electrode were also characterized. A linear stretching stage shown in Fig. 2(g) was used to apply tensile strain to a sample with PEDOT:PSS electrode, whose electrical resistance was measured under various levels of applied strain. As reported in our previous paper[6], the addition of salt could render the PEDOT:PSS electrode to become stretchable. This is confirmed by the results presented in Fig. 2(h), which shows that the resistance variation of the PEDOT:PSS electrode is less than 10 Ω under strain of up to 20%.

As shown in Fig. 3, the charge generation mechanism of porous PDMS TENG device can be explained by tribo-electrification and electrostatic effect[15, 19, 21] between tribo-positive PEDOT:PSS electrode and tribo-negative PDMS layer. Initially the PEDOT:PSS electrode is separated from non-porous PDMS surface by porous PDMS layer. When the TENG device is being pressed for the first time, PEDOT:PSS is brought into contact with non-porous PDMS surface, the friction of two materials causes the separation of triboelectric charges with different polarity, where positive charges accumulate on PEDOT:PSS and negative charges accumulate on non-porous PDMS surface due to different electron affinity of the material[22]. Under this situation, the negative charges on the non-porous PDMS is balanced entirely by the positive charges on top PEDOT:PSS electrode and electrostatic equilibrium is achieved. After the loading force is released, the deformed porous PDMS layer gradually restores to its original shape, giving rise to a large dipole moment through electrostatic effect, which resulting in an electrical potential difference created between the top and bottom electrode. Since the top PEDOT:PSS electrode has higher potential than the bottom electrode and two electrodes are connected through an external load, this potential difference would drive electrons to flow from bottom electrode to top electrode, generating electrical current in the load. When the TENG is pressed again, an inversed potential difference will be created between the two electrodes, which results in the transfer of electrons from top to the bottom electrode and generates current flow in the reverse direction. For the reference non-porous PDMS TENG, the charge generation mechanism is similar. However, compared with the porous PDMS, the non-porous PDMS layer has less frication area with PEDOT:PSS and higher Young's modulus, which leads to its different output performance from porous PDMS TENG.

For sandwich-structured TENG device working in contact-separation mode, the nanogenerator acts as both energy output device and energy storage device which operates similarly as a parallel-plate capacitor. The porous PDMS layer has lower elastic modulus than non-porous PDMS[19], and thus would exhibit larger displacement under the same compressive force, resulting in greater reduction in distance (Δd) between the two electrodes of the capacitor. Meanwhile, the dielectric constant of PDMS ($\varepsilon_{r\ PDMS} = 2.7$) is nearly three times higher than air ($\varepsilon_{r\ air} = \varepsilon_0 = 1$). When the porous PDMS layer is compressed, air will be expelled out of the porous layer and the deformed pores will lead to denser PDMS composition in porous layer and thus results in higher dielectric constant ($\Delta\varepsilon_r$). Therefore, with the same loading force and frequency, the change in capacitance of porous PDMS layer, expressed as $\Delta C_{porous} = \dfrac{\Delta\varepsilon_r}{\Delta d}\varepsilon_0 A$, would be greater than that of the non-porous PDMS layer $\Delta C_{non\text{-}porous}$.

Due to the existence of both porous PDMS layer and non-porous PDMS layer, the porous PDMS TENG could be considered as two parallel-plate capacitors in stack, where the top capacitor consists of PEDOT:PSS electrode/porous PDMS layer/non-porous PDMS surface and the bottom capacitor consists of non-porous PDMS surface/non-porous PDMS layer/metal electrode. In contrast, for the non-porous PDMS TENG, the capacitors are based only on non-porous PDMS layer. Assuming the negative charge density on non-porous PDMS surface saturates at a value of σ_N, those negative charges are being balanced by positive charges from both the top PEDOT:PSS electrode and the bottom metal electrode during the movements. The charge density on PEDOT:PSS electrode (σ_P) and metal electrode (σ_M) should satisfy

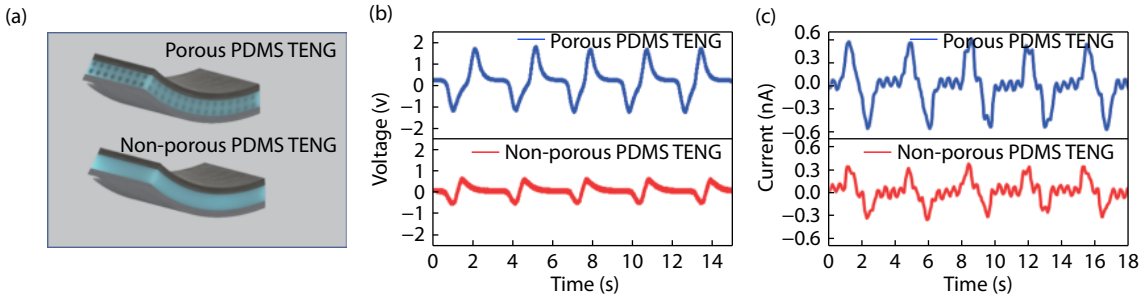

Fig. 4. (Color online) (a) Schematic illustrations of porous PDMS TENG (top) and non-porous PDMS TENG (bottom). (b) Output voltage and (c) output current of porous PDMS and non-porous PDMS TENG at loading force and frequency of 100 N, 0.8 Hz.

the relation of $\sigma_P + \sigma_M = \sigma_N$. According to the report by He *et al.* [21], σ_P is positively related to the capacitance (C_{top}) of top PDMS capacitor as $\sigma_P \propto C_{top}$. As discussed above, the top capacitor based on porous PDMS layer would undergo greater capacitance change ($\Delta C_{top\text{-}porous}$) compared to top non-porous PDMS capacitor of the non-porous PDMS TENG ($\Delta C_{top\text{-}non\ porous}$) when pressed and released at same loading force and frequency. This effect would lead to larger charge density change, represented by $\Delta\sigma_{P\text{-}porous} > \Delta\sigma_{P\text{-}non\ porous}$. When the top PEDOT:PSS electrode and bottom metal electrode are connected through an external load resistor, the output voltage and current generated can be expressed by the two equations below:

$$I(t) = -\frac{d\sigma_P}{dt}A, \tag{1}$$

$$V(t) = -\frac{d\sigma_P}{dt}A \times R_L, \tag{2}$$

where σ_P represents the charge density on the PEDOT:PSS electrode, A is the electrode surface area and R_L is the electrical resistance of the load resistor. The structural difference between the porous PDMS and non-porous PDMS TENG are illustrated in Fig. 4(a). To test and compare the performance of the porous PDMS and non-porous PDMS TENG, the electromechanical properties of both devices were measured. The loading force was exerted by a rubber pistol with a contact area of 6×6 mm^2 mounted on a horizontal-moving stepping motor that is carefully aligned with the PEDOT:PSS electrode of the nanogenerator. The nanogenerator devices were mounted on a stationary stage and a commercial force sensor (A502, Tekscan, Inc) placed behind the nanogenerator was used to precisely measure the magnitude and frequency of the applied force. Output voltage and current were both measured by a Keithley 2450 Source Meter. After the measurement, a low pass filter was applied to the output voltage and current data in MATLAB to filter out the noise. From the data presented in Figs. 4(b) and 4(c), one can see that when pressed under the same amount of loading force (100 N) and frequency (0.8 Hz), due to the larger change in charge density ($\Delta\sigma_P$) with the porous PDMS layer, the porous PDMS TENG exhibits larger average peak output voltage and output current at 1.65 V and 0.54 nA compared to non-porous PDMS TENG with 0.66 V and 0.34 nA. Furthermore, the improvement in output voltage and current might also be attributed to the increase in frictional area due to the larger surface-area-to-volume ratio offered by the porous PDMS structure, which could lead to larger charge density change as well[19]. From this point of view, the size of the pore could also play a role in enhancing the output performance of porous PDMS TENG. Although in this study only porous PDMS layer with pore size of 6 μm were fabricated, prior research by Lee *et al.*[19] has shown that the decrease of pore size would increase the output voltage and current due to the increased surface area-to-volume ratio.

The effect of loading force and loading frequency on the output of the TENG device has also been studied. Figs. 5(a) and 5(b) present the output voltage and current of the porous PDMS TENG under various loading force from 50 to 150 N. Lee *et al.* has previously reported that increasing the loading force would lead to an increase in output voltage[19]. This is because greater loading force could result in larger deformation in the PDMS layer, which would lead to larger capacitance change and thus higher output voltage. However, according to the results in Figs. 5(a) and 5(b), both the output voltage and current exhibit negligible amount of change under loading forces of 50, 100, and 150 N, suggesting that the porous PDMS is likely already fully compressed when the applied force exceeds 50 N and the output voltage and current have both reached their saturation values. Similar to the phenomena observed from piezoelectric and ferroelectret based nanogenerators[10, 23], the output voltage and current also increase with increasing loading frequency as shown in Figs. 5(c) and 5(d). This could be explained through Eqs. (1) and (2), from which one can see that higher loading frequency at given magnitude of force would result in an increased value of $d\sigma_P/dt$, thus resulting in larger output voltage and current.

4. Conclusion

In summary, we have demonstrated a porous PDMS film-based TENG device using intrinsically stretchable materials and a solution-based fabrication process. The formation of highly ordered, homogeneous porous PDMS structure has been confirmed by SEM and EDX and we have shown that the use of such porous PDMS could lead to TENG device with improved energy output (2.5 times improvement in output voltage and 1.6 times in output current) that outperforms similar device with non-porous PDMS. Its output responses to different loading force and loading frequency have also been studied to characterize the device and to explore its performance limitations for further improvements. The porous PDMS film processing method and the use of intrinsically stretchable electrode materials applied in this research might pave the way for the development of low-cost and

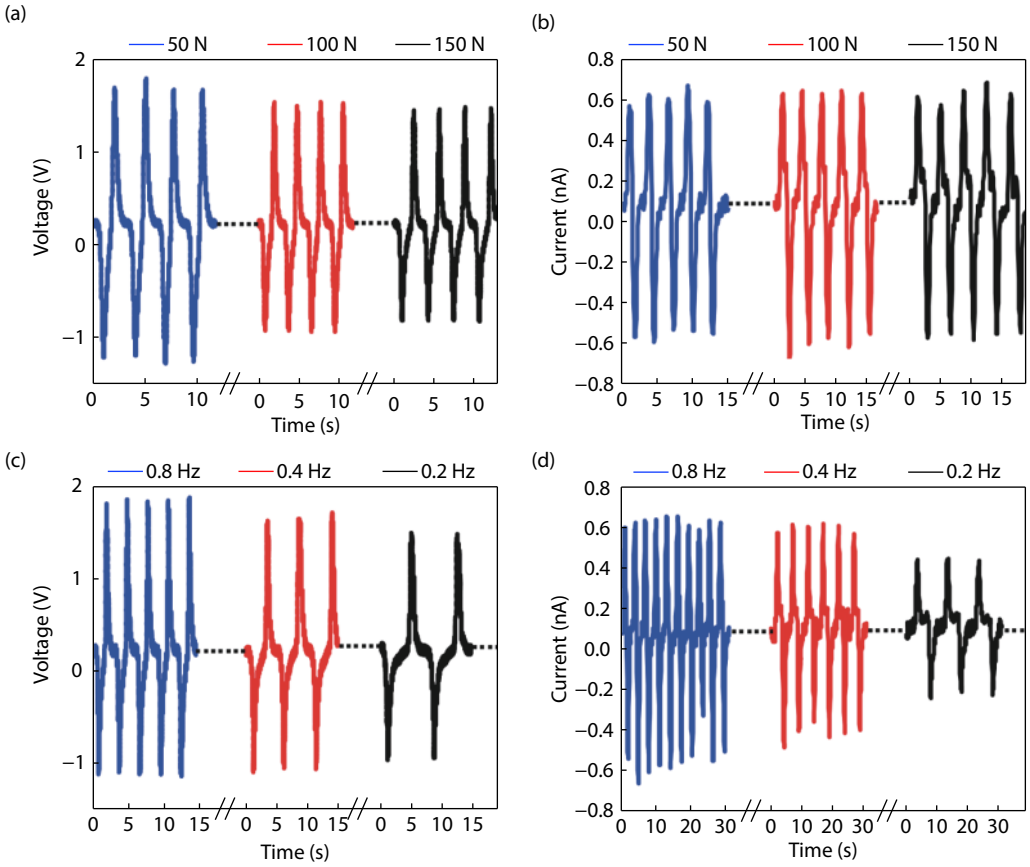

Fig. 5. (Color online) Loading force and frequency response of porous PDMS TENG. (a) Output voltage and (b) output current response under different loading forces at same loading frequency of 0.8 Hz. (c) Output voltage and (d) output current response under different loading frequencies at same loading force of 100 N.

large-area stretchable TENG for wearable electronics as self-sustained power source.

Acknowledgements

This work was partially funded by a Washington University Collaboration Initiation Grant (CIG) and a Michigan State University Foundation Strategic Partnership Grant (16-SPG-Full-3236).

References

[1] Wang C, Hwang D, Yu Z, et al. User-interactive electronic skin for instantaneous pressure visualization. Nat Mater, 2013, 12(10), 899

[2] Bade S G R, Shan X, Hoang P T, et al. Stretchable light-emitting diodes with organometal-halide-perovskite-polymer composite emitters. Adv Mater, 2017, 29(23), 1607053

[3] Cao X, Lau C, Liu Y, et al. Fully screen-printed, large-area, and flexible active-matrix electrochromic displays using carbon nanotube thin-film transistors. ACS Nano, 2016, 10(11), 9816

[4] Gao W, Emaminejad S, Nyein H Y Y, et al. Fully integrated wearable sensor arrays for multiplexed in situ perspiration analysis. Nature, 2016, 529(7587), 509

[5] Cai L, Zhang S, Zhang Y, et al. Direct printing for additive patterning of silver nanowires for stretchable sensor and display applications. Adv Mater Technol, 2018, 3(2), 1700232

[6] Shi H, Al-Rubaiai M, Holbrook C M, et al. Screen-printed soft capacitive sensors for spatial mapping of both positive and negative pressures. Adv Funct Mater, 2019, 29, 1809116

[7] Boutry C M, Beker L, Kaizawa Y, et al. Biodegradable and flexible arterial-pulse sensor for the wireless monitoring of blood flow. Nat Biomed Eng, 2019, 3(1), 47

[8] Kim Y, Chortos A, Xu W, et al. A bioinspired flexible organic artificial afferent nerve. Science, 2018, 360(6392), 998

[9] Yang R, Qin Y, Dai L, et al. Power generation with laterally packaged piezoelectric fine wires. Nat Nanotechnol, 2009, 4(1), 34

[10] Li W, Torres D, Wang T, et al. Flexible and biocompatible polypropylene ferroelectret nanogenerator (FENG): on the path toward wearable devices powered by human motion. Nano Energy, 2016, 30, 649

[11] Cao Y, Figueroa J, Pastrana J, et al. Flexible ferroelectret polymer for self-powering devices and energy storage systems. ACS Appl Mater Interfaces, 2019, 11, 17400

[12] Fan F R, Tian Z Q, Wang Z L. Flexible triboelectric generator. Nano Energy, 2012, 1(2), 328

[13] Zi Y, Guo H, Wen Z, et al. Harvesting low-frequency (< 5 Hz) irregular mechanical energy: a possible killer application of triboelectric nanogenerator. ACS Nano, 2016, 10(4), 4797

[14] Fan F R, Tang W, Wang Z L. Flexible nanogenerators for energy harvesting and self-powered electronics. Adv Mater, 2016, 28(22), 4283

[15] Chen J, Guo H, He X, et al. Enhancing performance of triboelectric nanogenerator by filling high dielectric nanoparticles into sponge PDMS film. ACS Appl Mater interfaces, 2015, 8(1), 736

[16] Zhu Y, Yang B, Liu J, et al. A flexible and biocompatible triboelectric nanogenerator with tunable internal resistance for powering wearable devices. Sci Rep, 2016, 6, 22233

[17] Wang S, Lin L, Wang Z L. Nanoscale triboelectric-effect-enabled energy conversion for sustainably powering portable electronics. Nano Lett, 2012, 12(12), 6339

[18] Fan F R, Lin L, Zhu G, et al. Transparent triboelectric nanogenerators and self-powered pressure sensors based on micropatterned

plastic films. Nano Lett, 2012, 12(6), 3109
[19] Lee K Y, Chun J, Lee J H, et al. Hydrophobic sponge structure-based triboelectric nanogenerator. Adv Mater, 2014, 26(29), 5037
[20] Wang Y, Zhu C, Pfattner R, et al. A highly stretchable, transparent, and conductive polymer. Sci Adv, 2017, 3(3), e1602076
[21] He X, Mu X, Wen Q, et al. Flexible and transparent triboelectric nanogenerator based on high performance well-ordered porous PDMS dielectric film. Nano Res, 2016, 9(12), 3714
[22] Chen X, Miao L, Guo H, et al. Waterproof and stretchable triboelectric nanogenerator for biomechanical energy harvesting and self-powered sensing. Appl Phys Lett, 2018, 112(20), 203902
[23] Dagdeviren C, Yang B D, Su Y, et al. Conformal piezoelectric energy harvesting and storage from motions of the heart, lung, and diaphragm. Proc Natl Acad Sci, 2014, 111(5), 1927